

# The STACEE Ground-Based Gamma-Ray Detector

D.M. Gingrich<sup>\*†</sup>, L.M. Boone<sup>‡‡‡</sup>, D. Bramel<sup>§</sup>, J. Carson<sup>¶</sup>, C.E. Covault<sup>||</sup>, P. Fortin<sup>\*\*</sup>, D.S. Hanna<sup>\*\*</sup>,  
J.A. Hinton<sup>††x</sup>, A. Jarvis<sup>¶</sup>, J. Kildea<sup>\*\*</sup>, T. Lindner<sup>\*\*</sup>, C. Mueller<sup>\*\*</sup>, R. Mukherjee<sup>§</sup>, R.A. Ong<sup>¶</sup>,  
K. Ragan<sup>\*\*</sup>, R.A. Scalzo<sup>††xi</sup>, C.G. Théoret<sup>\*\*xii</sup>, D.A. Williams<sup>‡</sup>, J.A. Zweerink<sup>¶</sup>

<sup>\*</sup>Centre for Subatomic Research, University of Alberta, Edmonton, AB T6G2N5, Canada

<sup>†</sup>TRIUMF, Vancouver, BC V6T2A3, Canada

<sup>‡</sup>Santa Cruz Institute for Particle Physics, University of California, Santa Cruz, CA 95064, USA

<sup>§</sup>Department of Physics and Astronomy, Barnard College and Columbia University, New York, NY 10027, USA

<sup>¶</sup>Department of Physics and Astronomy, University of California, Los Angeles, CA 90095, USA

<sup>||</sup>Department of Physics, Case Western Reserve University, Cleveland, OH 44106, USA

<sup>\*\*</sup>Department of Physics, McGill University, Montreal, QC H2A2T8, Canada

<sup>††</sup>Enrico Fermi Institute, University of Chicago, Chicago, IL 60637, USA

<sup>‡‡</sup>Present address: Department of Physics, The College of Wooster, Wooster, OH 44691, USA

<sup>x</sup>Present address: Max-Planck-Institut für Kernphysik, D-69029 Heidelberg, Germany

<sup>xi</sup>Present address: Lawrence Berkeley National Laboratory, Berkeley, CA 94720, USA

<sup>xii</sup>Present address: Laboratoire de Physique, Collège de France, F-75231 Paris CEDEX 05, France

**Abstract**— We describe the design and performance of the Solar Tower Atmospheric Cherenkov Effect Experiment (STACEE) in its complete configuration. STACEE uses the heliostats of a solar energy research facility to collect and focus the Cherenkov photons produced in gamma-ray induced air showers. The light is concentrated onto an array of photomultiplier tubes located near the top of a tower. The large Cherenkov photon collection area of STACEE results in a gamma-ray energy threshold below that of previous ground-based detectors. STACEE is being used to observe pulsars, supernova remnants, active galactic nuclei, and gamma-ray bursts.

## I. INTRODUCTION

Gamma-ray astronomy has become a very exciting area of research. Since 1991 the field has rapidly expanded due to the increased quantity and quality of data as well as an improved theoretical understanding of the related astrophysics. The thrust in the field was primarily initiated by NASA's Compton Gamma Ray Observatory (CGRO) and the ground-based detectors that ran concurrently. The Energetic Gamma Ray Experiment Telescope (EGRET) aboard the CGRO produced a catalog of over 200 high-energy point sources [1]. Since spaceborne instruments are by necessity small detectors, they are only able to detect sources below about 10 GeV. To increase the energy range, ground-based detectors must be used.

Almost all ground-based gamma-ray detectors use the atmospheric Cherenkov technique. Typical Cherenkov telescopes detect gamma rays by using large steerable mirrors to collect, focus, and image the Cherenkov light produced by the relativistic electrons resulting from the interactions of high-energy gamma rays in the upper atmosphere. This Cherenkov light is distributed on the ground in a circular pool with a diameter of 200 m to 300 m. Imaging Cherenkov telescopes have a very large collection area relative to satellite detectors, and need only capture a part of the total Cherenkov pool to detect the primary

gamma ray. This gives rise to a low-energy threshold of about 300 GeV.

The energy range between EGRET and imaging Cherenkov telescopes remained unexplored until recently because no detectors were sensitive to the region between 10 GeV and 300 GeV. The wavefront sampling technique is a variant of the imaging Cherenkov technique whereby the collecting mirror is synthesized by an array of large steerable mirrors (heliostats) at a central-tower solar energy installation. The large effective area of the collecting mirror allows one to trigger at lower photon densities, and therefore lower primary gamma-ray energies. STACEE is a wavefront sampling detector designed to lower the threshold of ground-based gamma-ray astronomy to approximately 50 GeV, near the upper limit of satellite detectors [2]. Three other projects of a similar nature have also been built: CELESTE [3], Solar-2/CACTUS [4], and GRAAL [5].

STACEE is investigating established and putative gamma-ray sources. One of its principle aims is to follow the spectra of active galactic nuclei (AGN) out to energies beyond that of EGRET measurements to determine where the spectra deviate from a power law. Many EGRET sources are not detected by imaging telescopes despite the fact that a simple extrapolation of EGRET spectra are often well within the sensitivities of such detectors. This effect could be due to cut-off mechanisms intrinsic to the source, or to absorption effects between the source and the detector. A likely absorption mechanism is pair production, wherein the high-energy gamma ray combines with a low-energy photon (optical or infrared) from the extragalactic background radiation field. Absorption by pair production thus makes gamma-ray measurements of distant sources an indirect method of measuring the integrated light from past star formation.

## II. STACEE DETECTOR

The STACEE detector was in a state of development from 1997 to 2002. Stages of the construction were followed by observing periods using the partially completed detector. Since the spring of 2002, the full detector has been completed and is begin used for astrophysical observations.

STACEE uses the National Solar Thermal Test Facility (NSTTF), which is situated at Sandia National Laboratories in Albuquerque, New Mexico (figure 1). Sixty-four of the 220 heliostats are used during clear moonless nights to collect Cherenkov light from air showers and direct it onto five secondary mirrors located near the top of a 61 m tower (figure 2). The secondary mirrors focus the Cherenkov light into groups of photomultiplier tubes (PMTs) such that each PMT views a single heliostat. Optical concentrators widen the aperture of each PMT and restrict its field of view to reduce the number of night-sky background photons detected. Signals from the PMTs are amplified and routed to a control room where high-speed electronics measure the charge and relative arrival times of the PMT pulses. Signals above threshold are discriminated and processed by a delay and coincidence trigger system.



Fig. 1. National Solar Thermal Test Facility at Sandia National Laboratories in Albuquerque, New Mexico.

### A. Heliostats

The choice of the 64 heliostats used in STACEE is based on the desire to uniformly sample the Cherenkov light pool expected from a shower impacting near the center of the array, while not crowding the PMTs in the image plane. The collective area of the 64 heliostats is over 2300 m<sup>2</sup>.

Each heliostat has a mirror area of 37 m<sup>2</sup>, and consists of 25 square facets mounted on a steel frame. Each facet is a 4 ft by 4 ft square of back-surfaced aluminized glass glued onto a thin metal sheet. The facets are distorted into approximately parabolic shapes with the focus set to be equal to the distance to the tower. Each facet can be separately aligned so that their beams overlap at the tower.

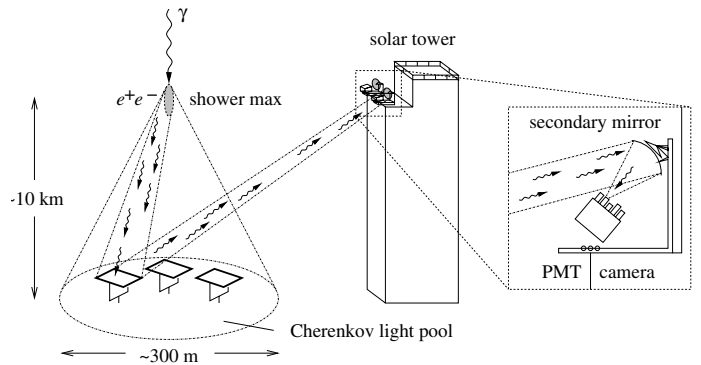


Fig. 2. Concept of the solar tower Cherenkov detection of gamma-ray air showers (not to scale).

The entire heliostat is mounted in a Y-shaped yoke structure which allows motion in the azimuth and elevation. The motion is achieved with two electric motors, each of which is controlled by the NSTTF central computer using 13-bit encoders.

Facet alignment is checked and tuned using images of the Sun projected onto the tower near solar noon (sunspots). The Sun is a good diagnostic since its angular size (0.5°) is very similar to that of a Cherenkov shower. The absolute pointing of each heliostat is calibrated to an accuracy of 0.05° using drift scans of bright stars.

### B. Secondary Mirrors

Cherenkov photons are reflected by the heliostats onto five secondary mirrors located near the top of the central tower. Sixteen heliostats in the north, 16 heliostats in the east, and 16 heliostats in the west regions of the field are viewed by three independent mirrors located 49 m above the base of the tower. Similarly, eight heliostats in the south-east and eight heliostats in the south-west of the field are viewed by two independent mirrors 37 m above the base of the tower.

The three secondary mirrors at 49 m are spherical with a nominal diameter of 1.9 m and a focal length of 2.0 m. Each is composed of seven identical hexagonal facets made from front-surfaced aluminized glass in order to retain a high reflectivity at ultraviolet wavelengths, where most of the Cherenkov light from air showers is produced. The two secondary mirrors at 37 m are single spherical mirrors with a diameter of 1.1 m and a focal length of 1.1 m.

The secondary mirrors focus the light from the heliostats, which arrives as a wide beam, onto phototube assemblies fixed in position at the focal plane. The optics are such that each heliostat is mapped onto a single PMT channel. This one-to-one mapping is vital for pattern recognition, which is used in trigger formation and background suppression.

### C. Cameras

The final stage in the STACEE optics chain is the camera. There is one camera for each secondary mirror. The cameras at 49 m consist of 16 PMT assemblies and the cameras at 37 m of eight PMT assemblies each. Each PMT assembly consists of a PMT and light concentrator enclosed in a cannister. The

PMT cannisters are mounted in cylindrical sleeves attached to an azimuthal-elevation mounting system secured to a slotted plate. With this system, it is possible to position the PMT cannisters anywhere laterally on the slotted plate and to adjust the orientation of the cannisters such that they point to the center of the secondary mirror.

The light concentrators are Dielectric Total Internal Reflection Concentrators (DTIRCs) [6] made from solid UV-transparent acrylic. These are non-imaging devices which use total internal reflection to transport light from the front surface to the exit aperture. The light from a circular area of 11 cm diameter is concentrated to an exit diameter of less than 4 cm. Only light from a given angular range can reach the exit aperture, so the DTIRCs have the added feature of being able to define the field of view of the PMT.

#### D. Photomultiplier Tubes

STACEE uses photomultiplier tubes with good sensitivity to short wavelengths (blue and UV), where most of the Cherenkov light is concentrated. Each PMT views the light from a 37 m<sup>2</sup> heliostat so it generates single photoelectrons from night-sky background at a rate in excess of 1.5 GHz. To reduce pulse pile-up effects, a PMT with a rapid rise time and narrow output pulse width was chosen. A small transit time spread is also desired since it results in better time resolution. Excellent time resolution allows us to exploit the narrowness of the Cherenkov wavefront at the trigger level to reject background from showers produced by charged cosmic rays. Offline, good timing resolution is valuable in reconstructing the shape of the wavefront (approximately spherical) in order to reject background.

The PMT used is the Photonis XP2282B with a borosilicate window and a VD182K/C transistorized voltage divider. Under typical operating conditions it has a rise time of 1.5 ns and a transit time spread of 0.5 ns.

The PMTs are supplied with high voltage from LeCroy 4032A high voltage power supplies, which are controlled by a LeCroy 2132 CAMAC interface in the control room. Voltages are typically in the neighbourhood of  $-1600$  V. The high voltage values are periodically adjusted to equalize the response of all channels.

#### E. Front-End Electronics

Signals from the phototubes are filtered and amplified near the cameras before being sent to the STACEE control room, located up to 18 m below the detector in the tower. There they are discriminated and used in trigger logic and timing measurements. Concurrently, the analog pulses are continuously digitized.

The front-end analog electronics are physically close to the PMTs. The PMT signals arrive at the front-end electronics via 11 m long RG58 cables. The signals passed through a high-pass RC filter having a time constant of 75 ns. This filter blocks any DC component of the PMT signal and removes slow PMT transients, which are not associated with Cherenkov signals.

The pulsed component of the signals exiting the filters are amplified by two cascaded fixed-gain (x10) wide-band

(275 MHz) amplifiers (Phillips Scientific 776). This amplification factor of 100 allows us to keep the PMT gain at approximately  $10^5$ , which is expected to prolong the life of the PMTs in an environment of high night-sky background light levels.

The filtered and amplified signals are routed through up to 40 m of low-loss coaxial cables (RG213) from the detector levels to the control room level of the tower where they are fed into linear fanouts (Phillips Scientific 748). The outputs of these fanouts are passed to the discriminators and flash ADCs (FADCs).

The analog signals from the PMTs are discriminated by 16 channel discriminators (LeCroy 4413 or Philips Scientific 7106) operating with a common threshold. The discriminator thresholds are set according to a rate versus discriminator threshold curve like the one shown in figure 3. In this plot, one sees data for in-time delays (circles) appropriate for Cherenkov triggers, and random delays (squares), which show the contribution from accidental coincidences caused by night-sky background photons. There is a breakpoint in the trigger rate, which is defined as the discriminator threshold below which the rate climbs exponentially. The location of the breakpoint depends on the individual channel rates, the widths of the discriminator pulses, and the number of channels required to form a trigger. At discriminator thresholds below the breakpoint, the rate is dominated by accidental coincidences. At very low discriminator threshold values the curve flattens due to deadtime. At discriminator thresholds above the breakpoint, the rate decreases slowly with discriminator threshold for in-time delays where the experiment is triggering mostly on Cherenkov light. In operating STACEE, the discriminator thresholds were set 15 mV to 20 mV above the breakpoint, which means there is very little background from accidental triggers.

#### F. Delay and Trigger System

A unique challenge in STACEE, that lead to the design of a custom-built delay and trigger system [9], is the requirement of dynamic delays. Due to the Earth's rotation, the gamma-ray source appears to move across the sky during the course of a night's observations. This effect continuously changes the relative arrival times of the Cherenkov photons at each heliostat. In order to maintain tight timing coincidences, signals from different channels are delayed by different amounts to correct for the source movement.

The programmable delay system has sufficient range to trigger on Cherenkov showers coming from any region of the sky within 45° of zenith. Individual delay settings can be controlled with a nominal precision of 1 ns. To ensure precise timing, every channel is calibrated with test pulses. The delays are updated every few seconds as STACEE tracks a source across the sky.

STACEE has a two-level trigger system. The 64 heliostats are divided into eight local subclusters of eight heliostats each. The discriminator outputs from the eight channels in each subcluster are routed through delays programmed to bring in-time hits into coincidence.

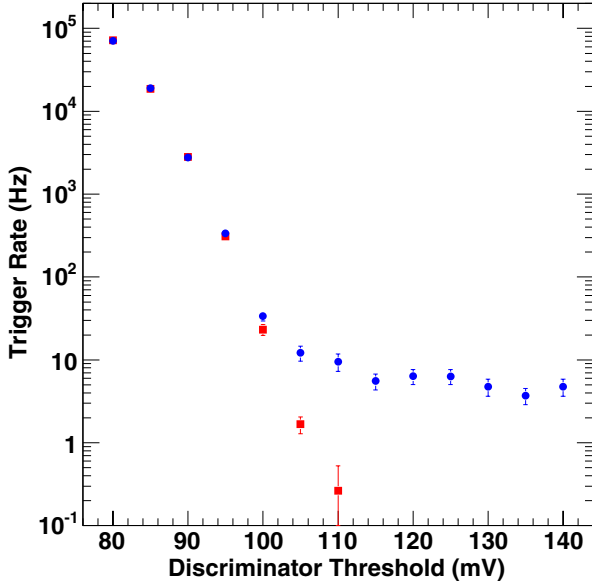


Fig. 3. Level-2 trigger rate versus discriminator threshold. The circles are data taken with in-time delays and the squares for random delays.

The number of coincident PMTs in a subcluster, and the number of coincident subclusters, are chosen to optimize the quality factor for the rejection of hadronic air showers according to Monte Carlo simulations. The discriminator threshold is then set at a level which makes the overall event trigger rate from chance coincidence of pulses due to fluctuations in the night-sky background photons negligible (less than  $0.2 \text{ min}^{-1}$ ).

Typical trigger settings are a discriminator threshold of 140 mV (about 5.5 photoelectrons), five out of eight PMTs are required to form a level-1 trigger, and five out of eight subcluster (level-1) triggers are required to form a level-2 trigger. The precise width of the subcluster coincidence window as applied to a given series of pulses varies between 8 ns and 24 ns due to the implementation of the trigger logic. The coincidence window for the level-2 trigger is 16 ns. The physical limit of the coincidence window is given by the intrinsic width of the Cherenkov wavefront of about 4 ns.

A by-product of the two level trigger system is that the light pool is required to be spread out over the entire heliostat array. This is a feature expected of showers due to gamma rays and is not a typical feature of showers initiated by charged cosmic rays.

The level-2 triggers are combined with fake trigger signals generated at a rate of 0.5 Hz. Fake triggers are used for determining individual channel rates and pedestal values. Whenever either type of trigger occurs (level-2 or fake), a common stop signal is sent to latch a GPS clock time and initiate the event read out. During readout, a veto is asserted to prevent the occurrence of additional triggers. The veto is cleared by the data acquisition (DAQ) program at the conclusion of readout.

Accidental triggers due to random night-sky hits in the

PMTs can be directly measured by using random settings for the programmable delays, which in effect is like pointing the heliostats in random directions.

### G. Flash ADC System

To reconstruct the energy and direction of the primary gamma ray, a commercial FADC system made by Acqiris Inc. is used. Sixteen channels of FADCs are contained in a special crate along with their own embedded computer running a version of the Linux operating system, modified to support real-time applications. Four FADC crates make up the system.

Each electronics channel is sampled at 1 GS/s with an 8-bit resolution and dynamic range of 1 V. The zero points of the FADC inputs are calibrated to a precision of 1 mV RMS, and the channel-to-channel gains of the system are equalized to within 0.5%.

The fully digitized PMT waveforms allow not only accurate measurements of the timing and intensity of the wavefront, but also the measurement of the charge-timing correlations, such as the distribution of Cherenkov photon arrival times at each heliostat. This enables us to use various new methods [7], [8] to reject the large background of hadronic events due to charged cosmic rays, while retaining gamma-ray initiated events.

### H. Laser Calibration System

STACEE is equipped with a laser calibration system comprising a 100  $\mu\text{J}$  nitrogen laser and dye cell feeding a network of optical fibres through a system of adjustable neutral density filters [10]. The fibres deliver light to the PMTs by exciting small diffuser plates attached to the center of the secondary mirrors. The intensity of each laser shot is measured independently using four PIN photodiodes.

### I. Miscellaneous Electronics

STACEE uses a GPS clock to provide a time-stamp, accurate to 1  $\mu\text{s}$ , for all recorded events. These time-stamps are necessary for pulsed emission searches.

Counters are used to measure the deadtime due to the read-out. Scalers are used to monitor the rates of all the discriminated PMT pulses as well as the level-1 subcluster triggers.

### J. Data Acquisition

The data acquisition system for STACEE is based on a VME embedded PC which reads out the VME crate and a CAMAC crate via a branch bus. Data is read out after each trigger and stored on local disks. At intervals, the data is copied from the local disks, along with the FADC data, to a PC and eventually written to DLT tape for archiving and off-site analysis. Monitoring in real time occurs on a PC running linux.

In the NSTTF control room, the positions and motions of the heliostats are monitored and the data is written to disk to be merged with the detector data at the end of an evening's observing. In a similar fashion the weather and atmospheric conditions are monitored and recorded.

### III. DETECTOR MODELING

The modeling of STACEE consists of simulating extensive air showers, the optical throughput of the detector, and the electronics. Since STACEE is an atmospheric Cherenkov experiment, the atmosphere is an integral part of the detector.

#### A. Extensive Air-Shower Simulations

The design and understanding of STACEE is aided by the CORSIKA air-shower simulation package [11]. CORSIKA makes use of packages such as EGS4 [12] and GHEISHA [13], which are widely used in other scientific fields. CORSIKA simulates the entire development of an extensive air shower, starting with the first interaction of the primary particle in the upper atmosphere, and follows all generated secondary particles until they reach the ground or their energy falls below the point where they no longer contribute to shower development. For the energies relevant to STACEE ( $E < 10^{12}$  eV) we are able to follow all particles since the multiplicities are small enough.

The intervening processes accounted for by the program include ionization, bremsstrahlung, and pair production, as well as effects such as the deflection by the Earth's geomagnetic field, and Coulomb scattering in the atmosphere.

The development of the shower depends on the density profile of the atmosphere, and thus an important input to the simulation is the assumed atmospheric profile. The rate and angle of production of Cherenkov photons by particles in the shower depend on the local refractive index. In addition, the attenuation of Cherenkov light due to Rayleigh and Mie scattering and absorption by oxygen allotropes are important simulated effects.

#### B. Optical Simulations

The second part of the STACEE simulation chain traces the optical path of Cherenkov photons through the detector optical elements. For this part, a custom-written ray-tracing package called "sandfield" (Sandia Field Simulator) was developed. Sandfield follows the path of every Cherenkov photon through the optical elements (heliostats, secondary mirrors, and DTIRCs) onto the PMT photocathodes, folding in transfer efficiencies at every stage. The arrival times are smeared with a Gaussian resolution of width 0.5 ns, which corresponds to the transit time spread of the PMT. The end result is a list, for each channel, of photoelectrons and their times of arrival at the PMTs. These lists are passed to the electronics simulator for further processing.

#### C. Electronics Simulations

STACEE PMTs are bombarded with a high flux of photons either from air showers or from night-sky background. The elevated rates caused by pile-up effects need to be understood quantitatively, so a detailed electronics simulation package is essential.

The photoelectrons from the air shower (generated by the sandfield program) are combined with random night-sky background photoelectrons generated uniformly in time according to Poisson statistics. A simulated analog waveform is built up by

superimposing single photoelectron pulses using an analytical pulse shape and adding them according to their arrival times.

The different gains of the channels are simulated by appropriate scaling of the pulse amplitudes. The waveforms are finally passed through a simulation of the discriminators.

#### D. Simulation Cross-Checks

In order to verify the simulations, calibration data is recorded and compared with the simulations. Detailed comparisons of CORSIKA with other air-shower simulations have been made. For sandfield, cross-checks have included simulating the sunspot data and the drift-scans of stars. For the electronics simulation, most quantities read out in the real data have been cross-checked, including PMT rates, distributions of FADC trace samples, pulse-height distributions, and the overall level-2 trigger rates, as functions of currents, gains, discriminator thresholds, etc.

### IV. SUMMARY

STACEE is a complete ground-based Cherenkov wavefront sampling gamma-ray telescope using heliostat mirrors of a solar energy research facility. Cherenkov light from air showers generated by the impact of high-energy gamma rays on the upper atmosphere is collected with a set of 64 heliostats with a collective area of over 2300 m<sup>2</sup>. To date STACEE has achieved a low-energy threshold of about 100 GeV, which is lower than previously obtained by ground-based imaging detectors. The complete detector has been operational since the spring of 2002, during which time observations of the Crab nebula, the active galactic nuclei 3C66A, OJ+287, W-Comae, Markarian 421 and H1426, and five gamma-ray bursts have been made.

### ACKNOWLEDGMENT

We are grateful to the staff at the National Solar Thermal Test Facility for their excellent support. This work was supported in part by the National Science Foundation, the Natural Sciences and Engineering Research Council, Fonds Québécois de la Recherche sur la Nature et les Technologies, the Research Corporation, and the California Space Institute.

### REFERENCES

- [1] R.C. Hartman *et al*, *Astrophys. J.* **123** (1999) 79.
- [2] D.S. Hanna *et al*, *Nucl. Instr. and Meth. Phys. Res.* **A491** (2002) 162.
- [3] M. de Naurois *et al*, *Astrophys. J.* **566** (2002) 344.
- [4] S.M. Tripathi *et al*, *BAAS* 34 (2002) 676.
- [5] F. Arqueros *et al*, *Nucl. Phys.* **B114** (2003) 253-257.
- [6] X. Ning, R. Winston and J. O'Gallagher, *Applied Optics* **26** (1987) 300.
- [7] R.A. Scalzo *et al*, *Proc. 28th International Cosmic Ray Conference*, Tsukuba, Japan, OG 2.5 (2003) 2799.
- [8] J. Zweerink *et al*, *Proc. 28th International Cosmic Ray Conference*, Tsukuba, Japan, OG 2.5 (2003) 2795.
- [9] J.-P. Martin and K. Ragan, *Proc. of the 2002 IEEE Nuclear Science Symposium*, 12, 141.
- [10] D. Hanna and R. Mukherjee, *Nucl. Instr. and Meth. Phys. Res.* **A482** (2002) 271.
- [11] D. Heck *et al*, *Tech. Rep. FZKA 6019*, Karlsruhe (1998); <http://www-ik3.fzk.de/~heck/corsika/>.
- [12] W.R. Nelson, H. Hirayama and D.W.O. Rogers, *SLAC-0265* (1985).
- [13] H. Fesefeldt, GHEISHA, the simulation of hadronic showers: physics and applications, (Aachen, Germany: Aachen, Tech. Hochsch., 1985).